JOURNAL OF MATERIALS SCIENCE 33 (1998) 4423–4433

Microstructure and crystal structure development in porous titania coatings prepared from anhydrous titanium ethoxide solutions

Y.-J. KIM, L. F. FRANCIS
Department of Chemical Engineering and Materials Science, University of Minnesota, Minneapolis, MN 55455, USA

Porous titania coatings were prepared by spin coating anhydrous titanium ethoxide–ethanol solutions in a controlled humidity atmosphere. Ti ethoxide reacted with atmospheric moisture during deposition, to form amorphous particles (approximately 200 nm), a dense layer or a combination of the two, depending on the processing conditions. Relatively humid atmospheres, low concentrations of Ti ethoxide in the coating solution and slow spinning rates favoured particle formation. These particulate coatings were typically composed of agglomerated particle clusters. Agglomeration could be prevented by adding hydroxypropyl cellulose to alkoxide solution to act as a steric stabilizer for newly formed particles. During thermal treatment, the coatings crystallized into the anatase phase and then transformed into the rutile structure at higher temperatures. The anatase–rutile transformation in porous coatings occurred over a range of 850–1150 °C and strongly depended on microstructural features. More porous coatings with larger particle clusters transformed to rutile at lower temperatures. Tensile stress in the coating caused by constrained shrinkage inhibited the phase transformation. The substrate constraint slowed the transformation rate in coatings relative to free powder. Stress relief through rupture of particle cluster connections allowed transformation to occur at lower temperatures. © *1998 Kluwer Academic Publishers*

1. Introduction

One advantage of chemical processing methods for ceramics is control of microstructure. In particular, the sol-gel method has been successful in tailoring the microstructure of ceramic coatings or thin films [1–3]. Pore content and pore size are often the microstructural features of interest as they influence many electrical, mechanical and chemical properties. For example, pores are essential for achieving good properties in titania membranes [4], catalyst supports [5] and gas sensors [6]. The scale of porosity most often studied in sol-gel derived coatings is on the nanometer level, i.e. 1–50 nm. Brinker and co-workers [7, 8] have shown how this fine porosity can be created by adjusting synthesis conditions to favour the growth of highly branched oligomeric structures that do not pack well during coating and resist collapse or even spring-back to highly porous structures during drying. Processing of coatings with larger pores has not received as much attention. For example, most reports for sol-gel derived titania thin films discuss the formation of "dense" microstructures or those having very small pores (<10 nm) [9–11]. Coatings with larger macropores (>100 nm) or broader pore size distributions are ideal for some applications, including gas sensors [12].

In previous papers [2, 13, 14], we described a "sol-to-precipitate" method for preparing macroporous titania coatings. An anhydrous titanium ethoxide solution is deposited by spin or dip coating; particles form by the reaction between Ti ethoxide in the solution layer and atmospheric water. These particles agglomerate and deposit onto the substrate, resulting in a porous coating with a range of pore sizes (0.1–3 μm). Transparent, non-particulate layers can be prepared by depositing anhydrous Ti alkoxide solutions in low humidity conditions [15, 16]. As described here, higher relative humidity conditions lead to microstructures in which the pore structure is determined by the packing of particles and agglomerates.

Particle formation in Ti ethoxide–ethanol–water solutions has received considerable attention [17–21]. The solution chemistry and precipitation conditions control the size and size distribution of hydrated titania particles that form in bulk solution. Zukoski and co-workers [19, 20] proposed that small particles (approximately 10 nm) nucleate after hydrolysis and condensation of the alkoxide, and then grow by an aggregative growth mechanism in which the small particles aggregate until they reach a stable size. For precipitation from low titanium ethoxide concentrations (<0.2 M), precipitated particles are stable and produce only small agglomerates of a few particles [19, 20]. The addition of polymer hydroxypropylcellulose; HPC [22, 23] or acids (hydrochloric acid or nitric acid [20]) to these solutions increases the

0022–2461

stability of precipitates and produces unagglomerated particles by steric and electrostatic hindrance, respectively. Since the same particle formation mechanism is at work in coatings, the results from bulk precipitation can be used to help improve coating microstructures.

In this report, we describe the effects of processing variables on microstructure and crystal structure development in porous titania coatings. In earlier work [2], we found that coatings prepared with higher spinning rates (or using solutions with a lower concentration of Ti ethoxide) had smaller particles and more compact particle clusters. Here, we define a processing window that allows porous particulate coatings to be prepared, more fully characterize the effect of processing variables (relative humidity, solution concentration, spinning rate), and discuss crystalline phase development and the phase transformation behaviour of the porous coatings.

2. Experimental procedure

2.1. Coating preparation and microstructure characterization

Coating solutions were prepared in a nitrogen glove box by combining titanium ethoxide, $Ti(OC_2H_5)_4$, with dry ethanol. Solutions were spin coated onto (1 0 0) Si or glass substrates using a photoresist spincaster (Headway Research, Garland, TX) in an atmosphere with controlled relative humidity (5–85% r.h.). To increase coating thickness, multiple depositions were used, with drying at 100 °C for 1 min between depositions. Multilayer coatings were heated in a box furnace to temperatures up to 1100 °C depending on the experiment, as specified below.

Two sets of experiments were carried out to determine the effects of processing variables on particle formation. First, a special deposition procedure was used to understand the effects of drying and reaction on the coating microstructure. Spin coating was carried out in an N_2 atmosphere to isolate drying from reaction (which requires water). Alkoxide solutions (0.5 M Ti ethoxide) were spin coated onto glass substrates under N_2 atmosphere; spinning was stopped after a specific time between 0.5 and 4.0 s, and the samples were then exposed to humid air (60% r.h.). After exposure to humid air for 5 min, coatings were dried at 100 °C for 1 min and the microstructure characterized by scanning electron microscope (SEM). In the second set of experiments, the three main processing variables were varied: the initial solution concentration (0.25–1.0 M Ti ethoxide), the spinning rate (2000–10 000 r.p.m.) and the relative humidity (10–80% r.h. at 22 °C). Coatings were prepared on Si (1 0 0) substrates and the microstructures were observed after drying by optical microscopy or SEM.

Coatings were also prepared from alkoxide solutions containing an electrostatic stabilizer (hydrochloric acid, HCl) or a steric stabilizer (hydroxypropyl cellulose, HPC, molecular weight of 100 000) to study agglomeration and porosity control in the coatings. Several solutions were prepared to provide a range of stabilizer concentrations (10^{-4}–10^{-2} M HCl and 10^{-4}–10^{-2} g HPC cm^{-3}). Solutions were spin coated on (1 0 0) Si substrates in humid atmosphere (40% r.h.). These coatings were heated at 500 °C between depositions. The higher temperature was necessary to pyrolyse HPC from the coating.

2.2. Pore content and size characterization

For a semiquantitative comparison of the pore content in the coatings, a thermogravimetric method [24] was used. The pore space of a coating (still on the Si substrate) was first filled with ethylene glycol by holding the coating in vacuum for 20 min and then soaking in ethylene glycol for 5 min. After carefully removing excess liquid, the sample was loaded into a thermogravimetric analyser (TGA; model TGA7, Perkin Elmer) and heated at 10 °C min^{-1} to 800 °C. The relative amount of porosity was determined from the weight loss data and the coating dimensions. A similar method has been successfully used to characterize the porosity of silica gels [25]. The average pore diameter in the titania coatings was measured from SEM photomicrographs by using a scanner and an image analysis program. The pore structure of several sets of coatings were characterized by these methods.

2.3. Anatase–rutile transformation

Coatings were prepared using a range of processing conditions to create a variety of microstructures; these coatings were all heated to 550 °C for 1 h to crystallize the anatase phase. The anatase–rutile transformation was characterized after these anatase coatings were heating isothermally for 1 h at temperatures of 700–1100 °C. The anatase–rutile phase transformation was investigated using X-ray diffraction (XRD, Seimens D-500). The relative amount of rutile was determined using the expression

$$\%\ \text{rutile} = \frac{I_{\text{rutile}(1\,1\,0)}}{I_{\text{anatase}(1\,0\,1)} + I_{\text{rutile}(1\,1\,0)}} \times 100 \qquad (1)$$

where $I_{\text{rutile}(1\,1\,0)}$ and $I_{\text{anatase}(1\,0\,1)}$ are the integrated peak heights of (1 1 0) peak for rutile and (1 0 1) peak for anatase, respectively. Microstructure development of coatings was studied using a field emission SEM (Hitachi S-900). Morphology changes by thermal treatment were observed in surfaces and cross-sections of coatings.

2.4. Stress measurement

The average stress in some coatings was analysed using a wafer bending method. Titania coatings were deposited on thin Si (1 0 0) wafers (75 μm thickness and 5 cm diameter: Virginia Semiconductor Inc., VA). Alkoxide solutions with initial Ti ethoxide concentrations of 0.5 and 1.0 M were spin coated at 2000 r.p.m. in a range of humid atmospheres (10–85% r.h.). Coatings were prepared with four depositions and drying at 100 °C. The coating thickness was determined by cross-sectional SEM of as-dried coatings. The curvature (or centre displacement) of wafers was measured

using a surface profilometer (Dektak IIA, Veeco Instruments) before and after deposition. According to a recommended procedure [26], the stylus is scanned over a length of 30 mm through the wafer centre with very small load. To avoid damage to the coatings, the back side of the wafer was scanned. Scans were taken three times with different directions and the centre displacement was taken as the average. The wafers were then heated to 300 °C for 1 h and the curvature measurement repeated. The procedure was repeated after heating at 550, 700, 800, 900 and 1000 °C. Average stress, σ, in the coating was calculated using a variation of an equation proposed by Stoney [27, 28]

$$\sigma = \frac{\delta}{r^2} \times \frac{E_s}{3(1-v)} \times \frac{d_s^2}{d_f} \quad (2)$$

where δ is the measured centre displacement; r is the radius of Si wafer (here, r is the half-length of the scanned distance, $r = 1.5$ cm); E_s and ν are Young's modulus and Poisson's ratio of Si ($E_s = 2 \times 10^5$ MPa, $v = 0.25$) respectively [29]; and d_s, d_f are the thickness of the Si substrate ($d_s = 75\,\mu m$) and the coating, respectively.

3. Results and discussion

3.1. Particle formation during deposition

Fig. 1 shows SEM photomicrographs of coatings prepared by spin coating in dry N_2 for a specific time and then exposing to humid atmosphere (55% r.h.) in stagnant conditions. For short spinning times (< 1.0 s), the solution layer dried only slightly and subsequent exposure to humid air led to the formation of particles. By contrast, coatings prepared using a longer spinning time (4.0 s) were thinner and had a higher Ti ethoxide concentration when exposed to humid air, resulting in a denser coating. Between these extremes, intermediate amounts of drying and reaction yielded coatings with microstructures containing both particulate and non-particulate components. The experiment not only verifies that the reaction of Ti ethoxide with water leads to the formation of particles, but also shows that this particle formation is sensitive to the Ti ethoxide concentration and hence drying. Beyond a critical

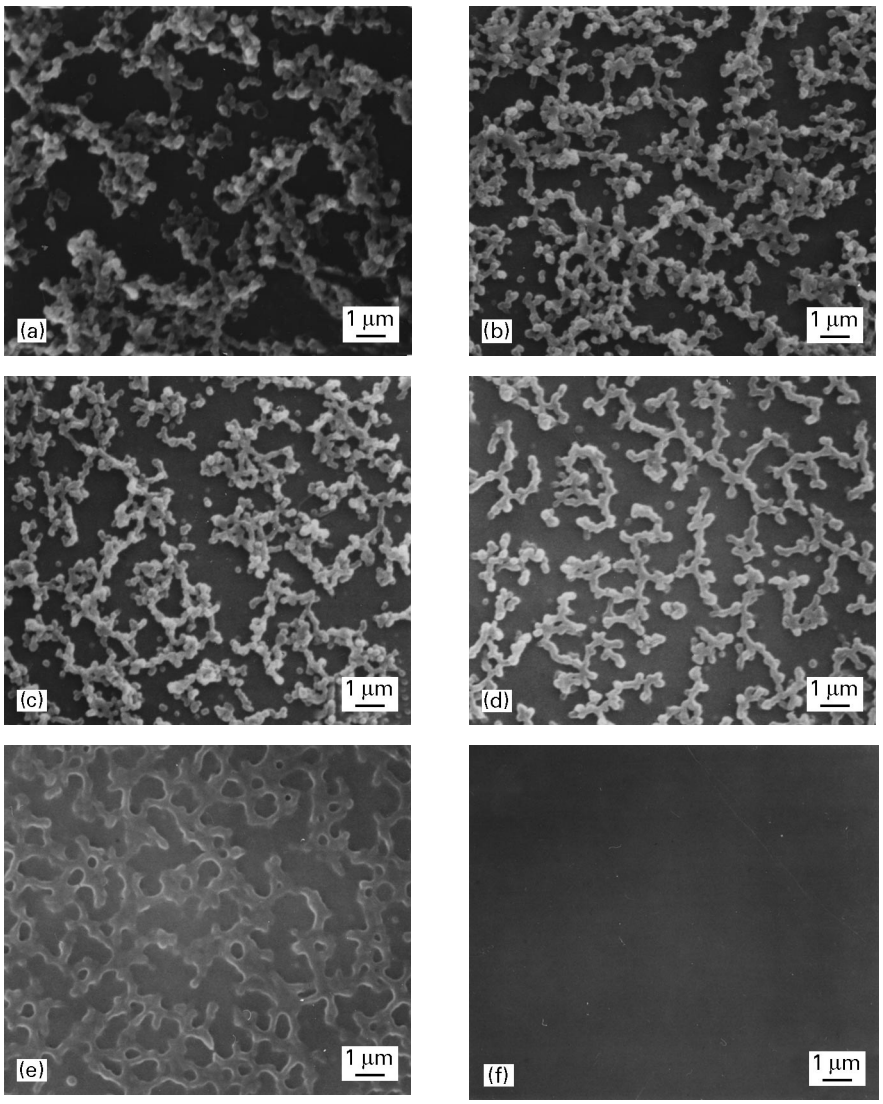

Figure 1 SEM photomicrographs of coatings spin coated under dry N_2 atmosphere for a specific time: (a) 0.5, (b) 1.0, (c) 2.0, (d) 2.5, (e) 3.0 and (f) 4.0 s, and then exposed to humid air (55% r.h.). Coatings were prepared using 0.5 M Ti ethoxide solution with 2000 r.p.m. and dried at 100 °C.

concentration, exposure to humidity leads to a dense layer without particles.

In normal coating conditions, drying and exposure to humid air occur simultaneously; therefore, the spinning rate, the initial solution concentration and the relative humidity impact particle formation. During spin coating, water enters the coating from the surrounding atmosphere and reacts with Ti ethoxide. Simultaneously, the concentration of Ti ethoxide in the deposited layer increases as ethanol evaporates. Microstructural features in the coating depend on the water content as well as the Ti ethoxide concentration. Fig. 2 shows particle formation maps for coatings prepared with a range of processing variables. Considering a solution with 1 M initial Ti ethoxide concentration (Fig. 2a), deposition at slow spinning rates and high relative humidity leads to particle formation. Under these conditions, drying is slow enough to allow time for water to enter the coating and react before the Ti concentration has increased beyond the critical limit. An increase in spinning rate decreases the tendency for particle formation, because drying is faster [30] and the concentration increases more rapidly. Decreasing the initial Ti concentration (Fig. 2b) allows a longer time to reach the critical concentration

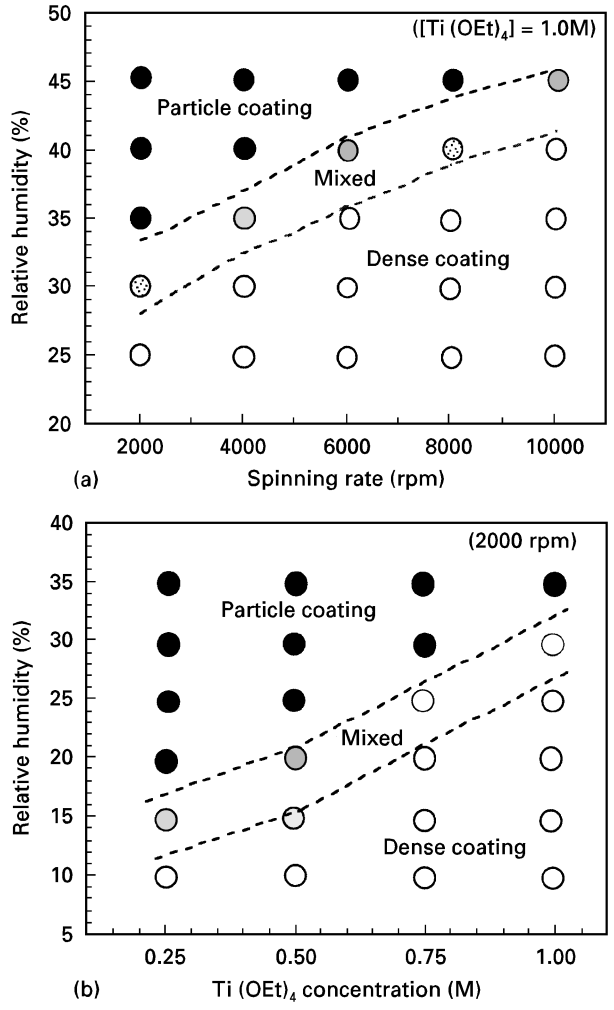

Figure 2 Particle formation maps for titania coatings deposited in a range of humid atmospheres: (a) effect of spinning rate (prepared with 1.0 M Ti ethoxide solutions) and (b) effect of solution concentration (prepared at 2000 r.p.m.).

and therefore enhances the tendency for particle formation. The relative humidity needed for particles to form is lower for less concentrated solutions. Even for conditions that favour particle formation, some of the alkoxide does not form particles, but instead deposits onto the particles and the substrate surface, presumably in the final stages of drying. Conditions resulting in "mixed" microstructures contained more of this non-particulate material.

The effects of processing variables on particle formation in coatings are consistent with research devoted to titania particle formation in bulk solution i.e. when a water–ethanol solution is mixed with a Ti ethoxide–ethanol solution. While the mechanism of particle formation is still a matter of debate, it is generally accepted that hydrolysis and condensation of the Ti ethoxide leads to the formation of small "primary particles" (diameter approximately 10 nm), which aggregate into larger particles. Particle formation depends on the hydrolysis ratio ($R = [H_2O]/[Ti]$). In these bulk solutions, typical conditions for particle formation are [Ti] = 0.05–0.2 M and $R > 3$; with more concentrated solutions, the alkoxide and water cannot be mixed homogeneously, and with lower R, only oligomeric species result [17–21]. For coatings, the initial solution is anhydrous; R depends on the water that enters the coating from the air and the concentration of Ti ethoxide. A simple analysis of the initial equilibrium between a humid atmosphere and a layer of ethanol shows that the mole fraction of water at the surface of the ethanol ($x_{water,\,s}$) increases linearly with the partial pressure of water (P_{water}) in the atmosphere, i.e. $x_{water,\,s} = HP_{water}$, where H is the Henry's law constant. Using partial pressure data [31], H is found to be 78.215 mm Hg. For the 0.25 M $Ti(OEt)_4$ solution, the particle formation map (Fig. 2b) shows that the relative humidity must be greater than 20% for particle formation. Ignoring the presence of Ti ethoxide (a 0.25 M solution contains only 5 vol% Ti ethoxide), we can use this analysis to predict the initial mole fraction of water at the surface as 0.051 (or a concentration of 0.91 M) which leads to an R of 3.6. This estimated value is sufficient for particle formation, according to the criteria established for bulk solutions. To form particles from solutions with higher initial concentrations of Ti ethoxide, higher relative humidity is needed in order to provide sufficient water to reach the needed R value (Fig. 2b). R is expected to vary through the coating thickness and fall as spinning proceeds due to evaporation of ethanol. Hence, particle formation is not likely in the later stages of drying, and non-particulate material forms on the substrate surface and over the particles. In addition to simply establishing the needed surface concentration of water, time is needed for the water to diffuse into the coating and for the particles to form. The effect of increasing the spinning rate for a given coating solution is to allow less time for these processes to occur and to accelerate the rise in the Ti ethoxide concentration during spin coating. Thus still higher relative humidity is needed to form particles at faster spinning rates (Fig. 2a).

3.2. Porous coating microstructure

Fig. 3 shows SEM photomicrographs of a titania coating prepared by spin coating Ti ethoxide solutions (1.0 M) in a high relative humidity atmosphere (70% r.h.). This coating microstructure contains features typical of coatings prepared using conditions that favour particle formation. The microstructure consists mainly of agglomerated clusters of particles with large pores between clusters and small pores within clusters. The size of the particle clusters changes with the coating conditions [2]. Low spin coating rates favour the formation of larger clusters (see Fig. 4). These larger clusters also tend to be less interconnected with only a few bridges to adjacent particle clusters. Likewise, for a given spinning rate, higher concentration solutions favour larger clusters. By contrast, coatings with smaller clusters form when higher spinning rates and less concentrated solutions are used. The contacts between particles contain necks or welds and a very thin, dense layer can be found at the substrate surface. For example, Fig. 3 shows a coating with a dense layer of 0.045 μm thickness on the substrate. The necks and dense layer originate from residual Ti alkoxide that does not form particles; such welds have also been observed for titania particles prepared from bulk solution [32]. The amount of the non-particulate material depended on the same processing parameters that control particle formation.

Fig. 5 shows the porosity and pore diameter of coatings prepared using a range of spinning rates. As

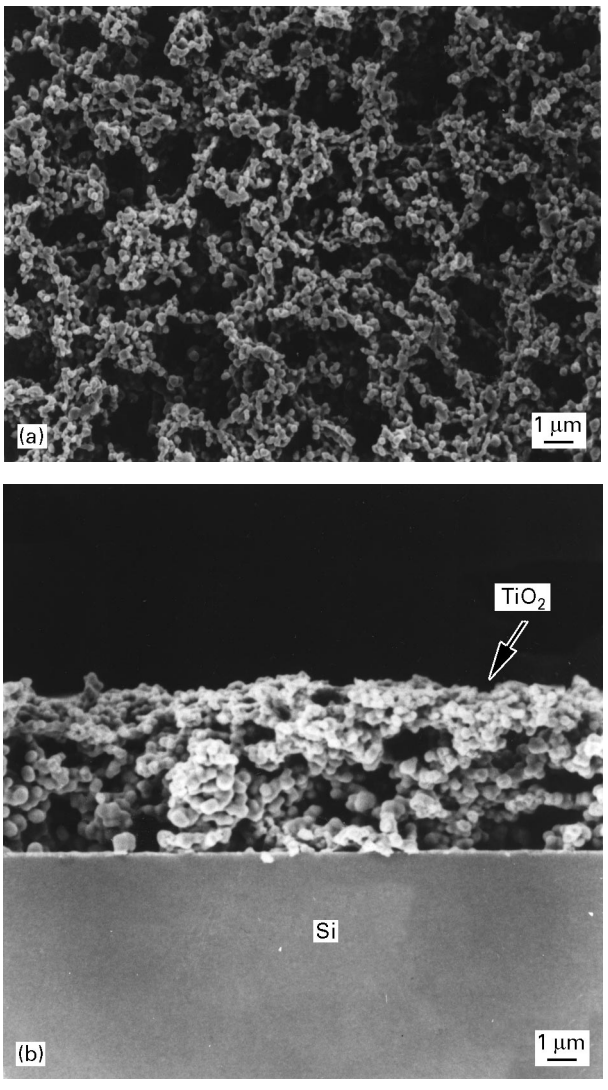

Figure 3 SEM photomicrographs of coatings prepared with eight depositions of 1.0 M Ti ethoxide solution (70% r.h., 2000 r.p.m.) and heated at 550 °C: (a) top view (b) cross-section view.

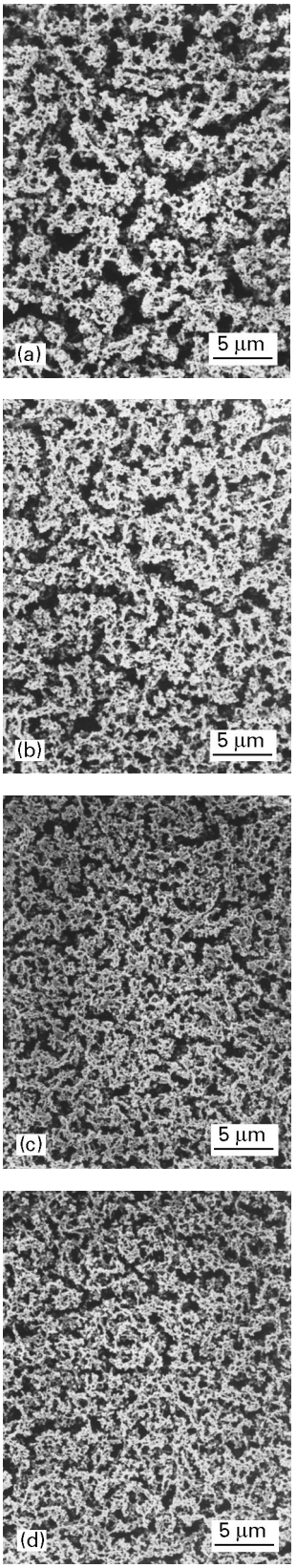

Figure 4 SEM photomicrographs showing the effect of spinning rate on coating microstructure: (a) 2000, (b) 4000, (c) 6000 and (d) 8000 r.p.m. All coatings were prepared with eight depositions of 1.0 M Ti ethoxide solution (70% r.h.) and heated at 550 °C.

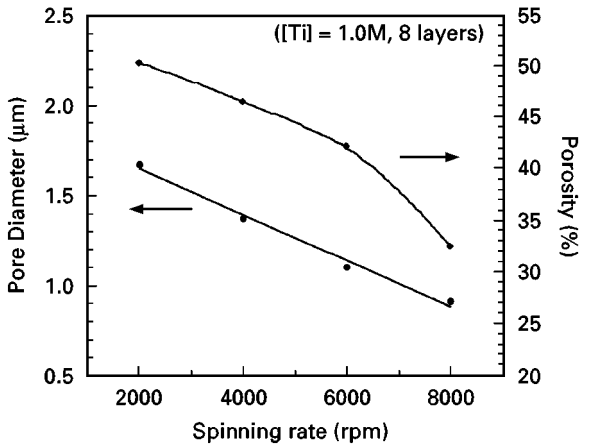

Figure 5 Effect of spinning rate on the porosity and pore size for coatings prepared with eight depositions of 1.0 M Ti ethoxide solution in humid atmosphere (70% r.h.) and heated at 850 °C.

the spinning rate increases, the per cent porosity and average pore size decrease from 51 to 32% and from 1.68 to 0.91 μm, respectively. The pore diameter in Fig. 5 refers to the average pore size of large pores between particle clusters. Small pores are also found within clusters (between individual particles). For example, the coating shown in Fig. 3 has an average large pore size of 1.68 μm with a range from 0.9 to 3.0 μm, and shows small pores having a size distribution between 0.1 and 0.5 μm. Pore size, size distribution and pore content of the coating depend on microstructural characteristics such as agglomerate size and particle size. Coatings prepared from solutions having higher Ti ethoxide concentration and using lower spinning rates are more porous with larger pores between clusters. The pore content and the pore size are determined by the nature of the clusters that form as particles agglomerate during coating.

The addition of stabilizing additives to alkoxide solutions prevented agglomeration and resulted in less porous coatings. Fig. 6 shows SEM photomicrographs of coatings prepared by spin coating 0.2 M Ti ethoxide solutions without additives, with HCl and with hydroxypropyl cellulose (HPC). The addition of HCl as an electrostatic stabilizer was not very effective; only a narrow range of HCl helped to prevent agglomeration of particles ($0.75–1.5 \times 10^{-3}$ M for 0.2 M Ti solution and 40% r.h.). The addition of HCl above and below this concentration range resulted in a dense gel-like coating. By contrast, coatings prepared with HPC have less agglomerated particles and smaller pores. The coating prepared with HPC has a lower porosity and has more uniform pore size distribution as compared with unmodified coatings. For example, the thicker coating shown in Fig. 7 has 28% porosity and pores in the range of 0.1–0.2 μm. This pore content is about 15% lower than that of an identically prepared coating prepared without HPC. HPC is effective over a wide concentration range, but only with solutions with lower Ti alkoxide concentrations (<0.3 M). Coatings prepared with HPC required a thermal treatment of 500 °C between depositions to remove the HPC; without the thermal treatment multilayer coatings were agglomerated.

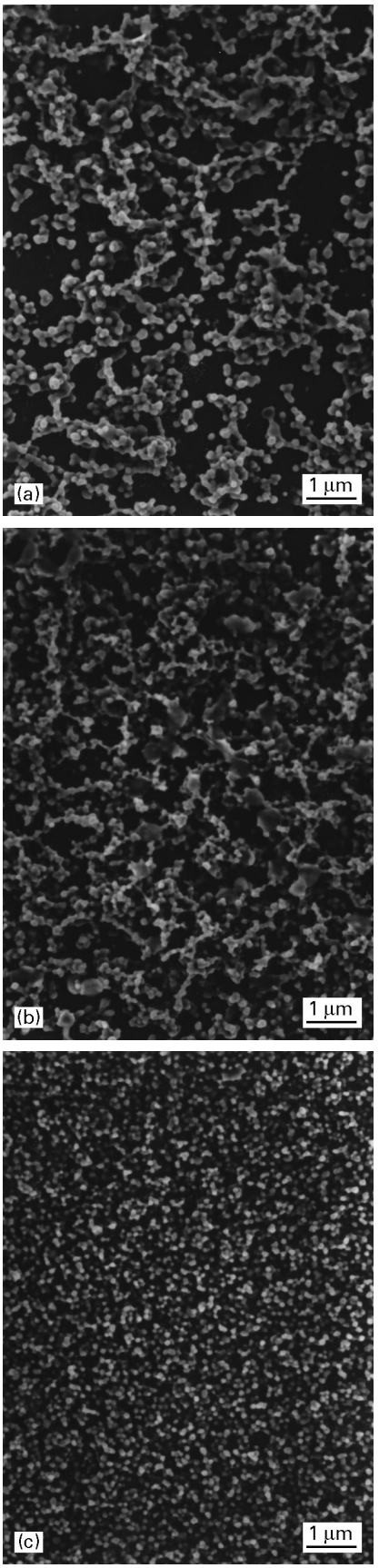

Figure 6 SEM photomicrographs of coatings prepared from 0.2 M Ti ethoxide solution (a) without any additives, (b) with HCL (1.0×10^{-3} M), and (c) with HPC (3.0×10^{-3} g cm^{-3}). Coatings were prepared with five depositions at 2000 r.p.m. in humid air (40% r.h.) and heating at 500 °C between depositions.

The factors that influence particle formation discussed in the last section also control the microstructural features in porous coatings, e.g. cluster size, pore

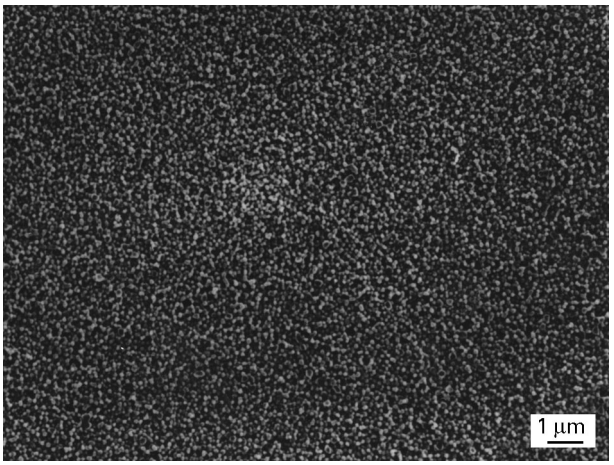

Figure 7 SEM photomicrograph of a coating prepared with 16 depositions of a 0.2 M Ti ethoxide solution containing HPC (1.7×10^{-3} g cm^{-3}) and heated at 500 °C for 5 min between depositions.

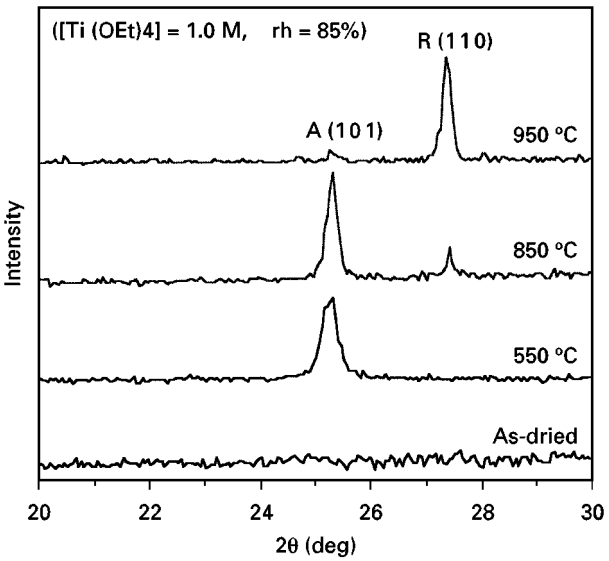

Figure 8 XRD data showing the effect of heat treatment on phase transformation of a coating prepared with four depositions using 1.0 M Ti ethoxide solution (85% r.h., 2000 r.p.m.).

size, porosity. Cluster sizes are determined by the particle–particle separation distance and the time available for agglomeration during the coating process. Cluster size is smaller for solutions with low alkoxide concentrations because the newly formed particles are further apart and require more time to agglomerate. Also, for a given alkoxide concentration, clusters are smaller for faster spinning rates as less time is available for agglomeration and the shear associated with faster spinning enhances agglomeration [19]. Those coatings containing smaller clusters tend also to be more dense as the smaller clusters pack more effectively.

3.3. Anatase–rutile transformation

Fig. 8 shows XRD data for a porous titania coating after different thermal treatments. As-deposited, the coating is amorphous. Complete crystallization to the anatase phase occurs after the 550 °C thermal treatment, with transformation to rutile requiring higher temperatures. For this coating, the transformation is nearly complete after the 950 °C thermal treatment. Fig. 9 shows the microstructure change during thermal treatment up to 900 °C. After heating at 550 °C, precipitated particles (approximately 150 nm) consist of small anatase grains (approximately 10 nm). After heating at 750 and 850 °C, XRD shows that the material is still anatase; however, the small grains have grown to 30 and 50 nm, respectively. When the phase transformation to rutile is nearly complete (after heating at 900 °C), the microstructure consists of rutile grains with a size similar to that of the original precipitated particle (approximately 150 nm). This change is microstructure along with crystal structure is consistant with the observations of other researchers [33].

Processing variables that affect the coating microstructure, i.e. the spinning rate, relative humidity, Ti ethoxide concentration, have a strong impact on the phase development. To study the anatase–rutile transformation, coatings were prepared under a variety of conditions and all were heated to 550 °C for 1 h to produce anatase. Then, the anatase coatings were heated to various temperatures for 1 h and XRD was used to determine the extent of transformation.

Fig. 10 shows the effects of the Ti ethoxide concentration in the coating solution and the spinning rate on the anatase–rutile transformation in porous coatings. Relative humidity conditions were held constant at a level (55%) that caused all coatings to be particulate. Coatings prepared with a lower spinning rate (see Fig. 10a) and from more concentrated solutions (see Fig. 10b) transformed to rutile at lower temperatures. These coatings had more porous microstructures with large clusters and larger individual particles (see Figs 3 and 4 and references [2, 14]), and they were thicker. Coatings that required higher temperatures for transformation were those that were denser and had smaller individual particles and clusters; these coatings were also thinner. Dense coatings prepared under conditions that do not give rise to particle formation (not shown) remained in the anatase phase even after extended heating at 1100 °C.

Since the data presented in Fig. 10 reflect the influence of both thickness and microstructure, additional experiments were carried out to try to separate these effects. Coatings were prepared with identical thickness, but different microstructures; microstructure was controlled by solution concentration and thickness by the number of depositions. Fig. 11a shows that coatings with denser microstructures (prepared from less concentrated solutions) do not transform as easily. The transformation in coatings with varying thickness, but similar microstructure, was compared with a free powder. Powder was prepared by precipitating in humid air (85% r.h.) without spinning, and coatings were spin coated (in humid air, 85% r.h.) with four and ten layers deposited. While titania powders have almost completely transformed to rutile phase after heating at 850 °C, coatings are still mostly anatase after the same thermal treatment (see Fig. 11b). The thinner of the two coatings contained less rutile. These

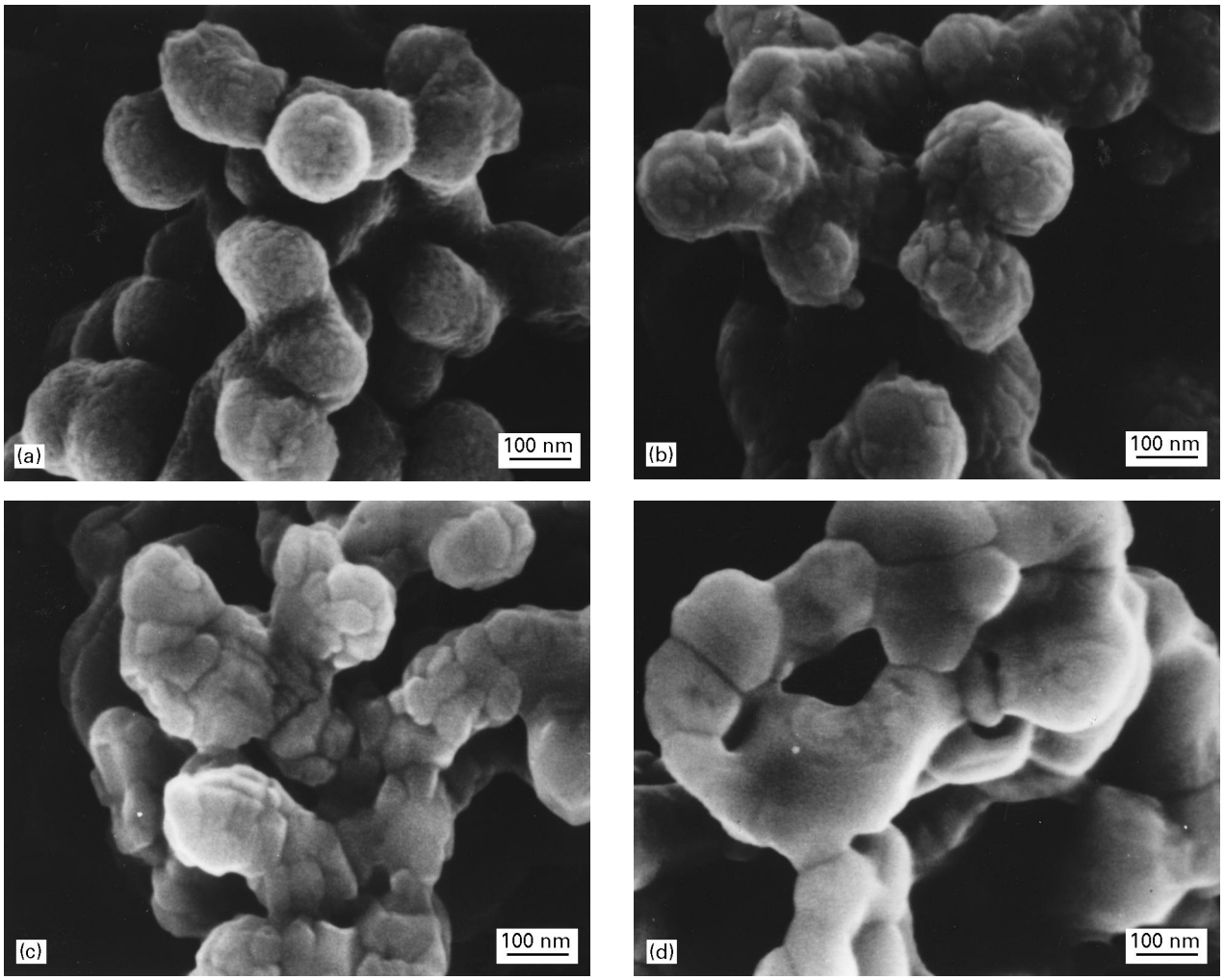

Figure 9 SEM photomicrographs for titania particles in porous coatings heated at a range of temperatures for 1 h: (a) 550 °C, (b) 750 °C, (c) 850 °C and (d) 900 °C. Coatings were prepared with four depositions using 1.0 M Ti ethoxide solution (85% r.h., 2000 r.p.m.).

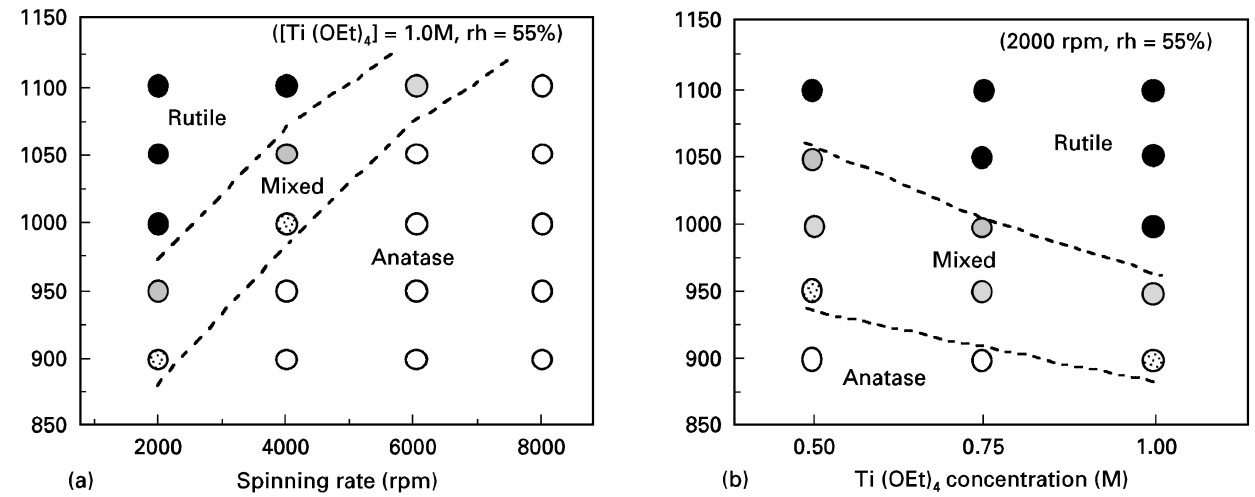

Figure 10 Phase transformation maps showing effects of (a) spinning rate and (b) concentration of Ti ethoxide in the coating solution on the anatase–rutile transformation behaviour. Coatings were prepared with four depositions in humid air (55% r.h.), followed by heating for 1 h at 550 °C to crystallize anatase and then heating at various temperatures for 1 h. Data based on XRD results.

data show that both coating thickness and microstructure influence the transformation behaviour.

Rutile is the thermodynamically stable crystalline form of titania. Titania prepared at low temperatures by methods such as sol-gel typically crystallizes first into the anatase phase. Since anatase is metastable, the transformation to rutile is irreversible and has been reported to occur over a wide range of temperatures (approximately 400–1200 °C), as recently reviewed by Kumar *et al.* [34]. In bulk sol-gel derived titania, the

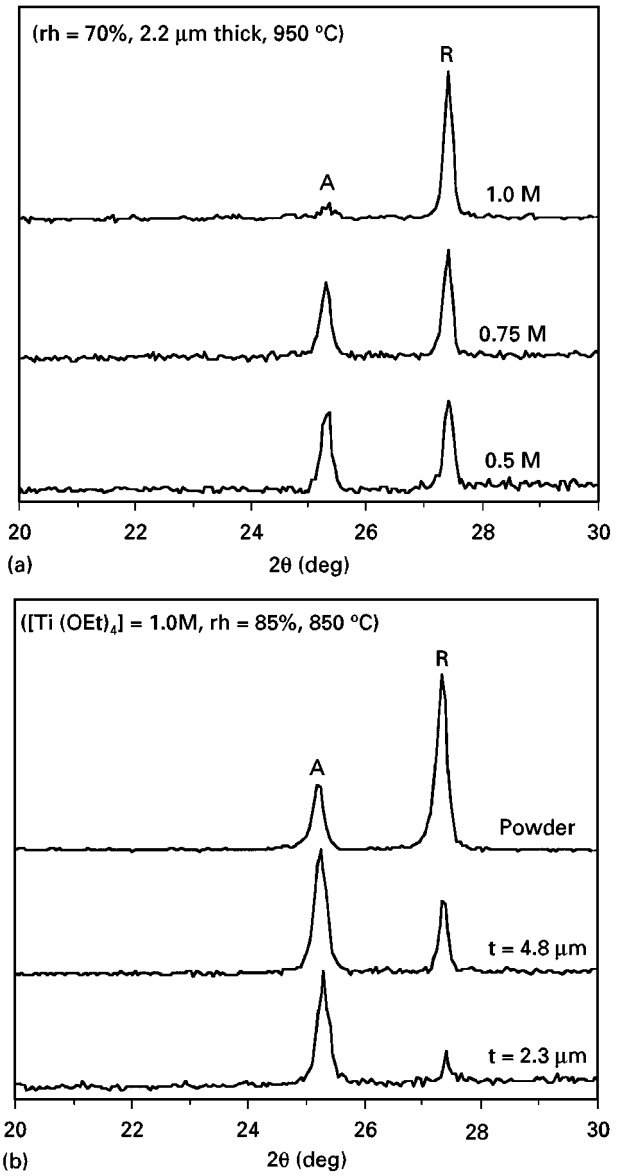

Figure 11 XRD results showing comparisons of: (a) coatings with different microstructure but similar thickness (2.2 μm) and (b) titania powder and coatings with different thicknesses (see text for explanation).

transformation depends on the method of preparation and has been reported to be affected by the extent of dilution [35] and particle size and coordination [33]. In coatings, the transformation behaviour also depends on the method of preparation and has been reported to depend on heating rate [36]. Titania membranes that are prepared on a porous support transform slower than unsupported membranes due to the constraint of the support [35]. The transformation from anatase to rutile requires an 8% decrease in volume. In a coating adhered to a substrate, this volume change is constrained by the substrate and an in-plane tensile stress develops in the coating [37]. Other constrained volume changes from drying, crystallization, sintering and thermal expansion mismatch also lead to stresses in coatings. Stress measurements were carried out on our coatings in order to understand better the effect of microstructure and thickness on the transformation.

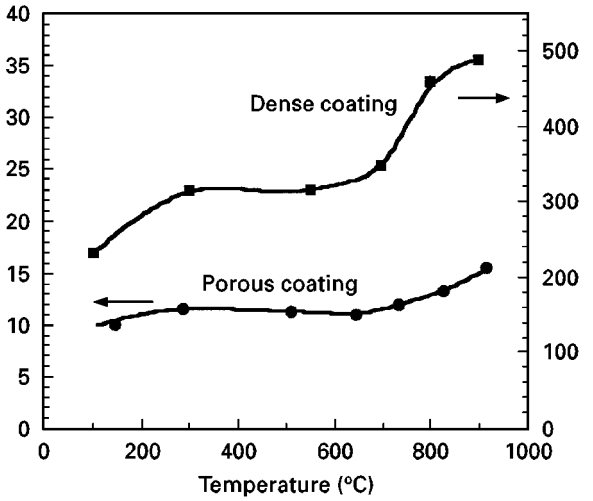

Figure 12 Effect of heating temperature on the residual tensile stresses of a porous and a dense coating deposited on a thin Si wafer. The porous coating (2.3 μm) was prepared using four depositions of 1.0 M Ti ethoxide solution at 2000 r.p.m. in humid air (85% r.h.). The dense coating ($t = 0.06$ μm) was prepared by one deposition of a 0.5 M Ti ethoxide solution at 5000 r.p.m. in dry air (10% r.h.).

Fig. 12 shows the stress measured at room temperature for a porous coating and a dense coating after heating to various temperatures. After drying at 100 °C, the porous amorphous coating has an average tensile stress of 10.2 MPa; this stress is likely due to constrained shrinkage during drying. Heating to higher temperatures (200–700 °C) increases the stress slightly. In this temperature range, a tensile stress from the crystallization of anatase is expected, but stress relaxation is also possible. The stress rises more significantly at higher temperatures, reaching 16 MPa after the 1000 °C heat treatment. The coating completely transforms to rutile (by XRD) in this temperature range. Surprisingly, the stress development is modest despite the large volume change from the transformation. The stress in a dense, non-particulate coating (prepared using low r.h. conditions) is very large although this coating does not transform to rutile. Stresses in the dense coating are associated with constrained shrinkage from solvent loss after solidification, densification and crystallization to anatase.

These stress results can be interpreted using a general expression for the stress in an elastic coating. Considering a biaxial plane strain, the stress in the coating, σ, is given by

$$\sigma = \frac{E\varepsilon}{1 - \nu} \tag{3}$$

where ν and E are the Poisson's ratio and the elastic modulus of the coating, respectively; and ε is the isotropic linear strain in the coating [37]. Since the coating stress is directly proportional to the coating elastic modulus, porous coatings will develop a lower stress for a given amount of strain. The modulus effect was, in part, responsible for the differences in stress between porous and dense coatings in this study. The other factor affecting stress is coating strain, which is related to constrained volume change. The isotropic

linear coating strain is one-third of the fractional constrained volume change, $\Delta V/V$. Solvent departure after solidification, crystallization, sintering and phase transformation to rutile all involve shrinkage and impart a contribution to tensile stress. Thermal expansion mismatch between Si ($\alpha = 2.6 \times 10^{-6}\,^{\circ}C^{-1}$) and anatase ($\alpha = 4.8 \times 10^{-6}\,^{\circ}C^{-1}$) causes a compressive contribution to the stress on heating (thermal strain $= \Delta\alpha\Delta T$) and a tensile contribution on cooling. If no change in the thermal expansion coefficient or elastic modulus of the coating takes place during the heat treatment, this stress is reversible. The thermal expansion coefficient of the amorphous phase is likely higher than that of crystalline titania and thus some compressive contribution to stress will remain after cooling when the material first crystallizes. Increases in the elastic modulus during a thermal treatment, i.e. due to sintering, will result in a tensile contribution to the stress at room temperature. A very significant contribution to coating stress is expected for transformation to rutile. The 8% volume change ($\varepsilon = 0.0267$) associated with the transformation to rutile in a porous coating ($E \approx 0.2\,E_{\text{rutile}} = 50$ GPa; $\nu = 0.33$) should result in a tensile stress in excess of 2 GPa. Clearly, there must be some mechanism of stress relaxation or relief in the porous coatings that transform to rutile.

Fig. 13 shows a SEM photomicrograph of the coating prepared from 1.0 M Ti ethoxide solution and heated at 550 °C. Some of the connections between particle clusters are broken. The tensile stress in the coating arising from drying, densification and crystallization was high enough to break these particle connections. The stress is lowered because individual disconnected clusters can shrink more freely, especially near the surface. The large strain involved with the transformation to rutile can then be accommodated. Denser coatings have smaller, more well connected clusters, which cannot break, and consequently their conversion to rutile is inhibited and final stress is higher.

The substrate constraint on the transformation is expected to be greatest near the substrate and least at the surface. The variation in rutile content through the thickness of the coating was determined by filling the pore space with epoxy and taking XRD data periodically as the coating was ground away with sandpaper. Fig. 14 shows the XRD data for a partially transformed coating. The relative amount of rutile phase decreased from 70 to 20% as grinding proceeded. The gradient in crystal structure is caused by a microstructure and stress gradient through the thickness, with low stress (due to broken connections) and easy transformation on top and high stress (due to substrate constraint) and low rutile content nearer to the substrate.

With the stress data and microstructure observations, the transformation behaviour of the coatings in this study can be explained. Since the coating can only shrink in the thickness direction, the adherence to the substrate requires that a large tensile stress accompany the transformation. The substrate constraint slows the rate of phase transformation in coatings in much the same way as sintering of particulate coatings is slower than in bulk ceramics [38]. Additionally, the tensile stress that develops from constrained shrinkage before the transformation opposes the transformation; this stress depends on the amount of shrinkage, the coating modulus and the stress relaxation. Porous coatings with loosely connected particle clusters have low modulus and have the ability to fracture and relax the stress. These coatings develop smaller stresses and can accommodate the transformation strain; therefore, porous coatings are able to transform completely to rutile. Denser, stiffer coatings develop larger stresses and hence require higher temperatures to transform. Coincidentally, conditions that lead to higher density also lead to smaller individual particles in the clusters; there is evidence that smaller particles also inhibit the transformation [35]. The strong effect of thickness on transformation (in coatings with constant particle size and co-ordination number) leads to

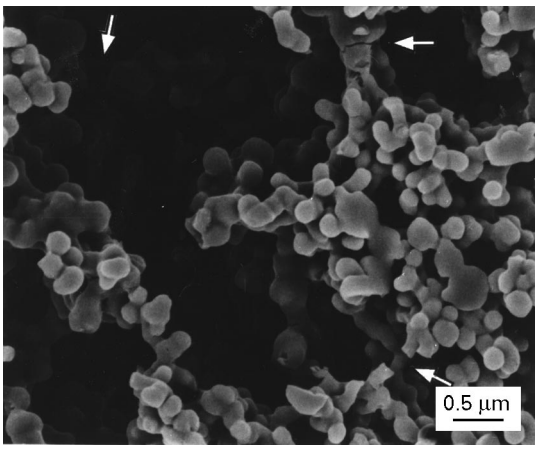

Figure 13 SEM photomicrograph showing broken connections between particle clusters in porous coatings heated at 550 °C. The coating was prepared using four deposition of a 1.0 M Ti ethoxide solution at 2000 r.p.m. in air (85% r.h.).

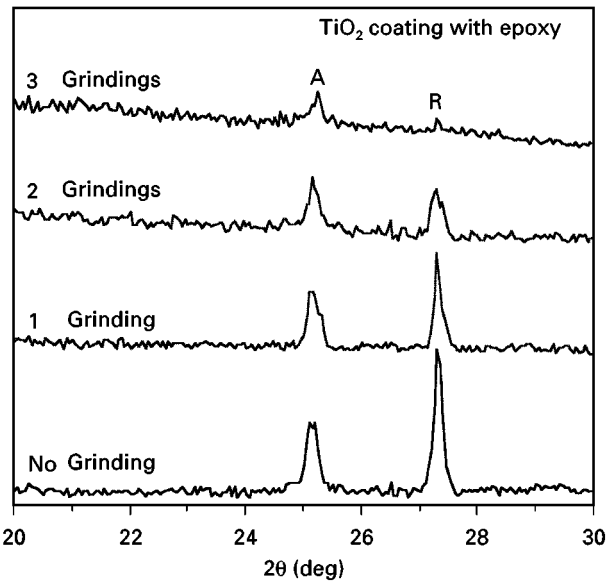

Figure 14 XRD results showing a crystal structure gradient through the thickness of a porous coating heated at 950 °C. The porous titania coating was filled with epoxy and investigated crystal structure repeatedly after grinding from the top surface.

the conclusion that the substrate constraint is the most important factor governing the transformation behaviour for these coatings.

4. Conclusions

Particle formation in coatings deposited from Ti ethoxide solutions is a strong function of the alkoxide concentration, the spin coating rate and the relative humidity. For particles to form, enough water must enter the coating from the atmosphere to create a water–alkoxide ratio above approximately three and time must be available for the water to diffuse into the coating and for particles to form. When the alkoxide concentration in the layer is too high, these conditions are not met and a dense layer, rather than particles, forms. Starting with a low concentration of alkoxide in the coating solution and using a slower spinning rate allows more time before the alkoxide concentration becomes too high; hence particle formation is favoured so long as the relative humidity is high enough. Particle formation maps were presented here to document the range of processing conditions that result in particulate coatings.

The microstructure of the particulate coatings was macroporous with average pore sizes in the range 0.1–3 μm; porosity was created by packing of particle clusters. Particle cluster size increases as the particle–particle seperation distance decreases (lower alkoxide concentrations) and the time available for agglomeration increases (faster spinning rates). Particle clusters could be eliminated by adding HPC to the alkoxide solution to act as a steric stabilizer for newly formed particles. Coatings prepared with HPC were denser and had narrower pore size distributions. Thermal treatment led to the crystallization of anatase and then at higher temperatures to a transformation to rutile. Since the anatase–rutile transformation requires an 8% volume shrinkage, the substrate constraint slowed the rate of phase transformation in the coatings. Only coatings with microstructures consisting of porous, loosely connected clusters were able to transform; these coatings released some of the tensile stresses through rupture of connections between particle clusters.

Acknowledgements

This material is based upon work supported by the US Army Research Office under contract/grant number DAA3-92-0274. We thank also the NSF Center for Interfacial Engineering for use of its characterization facility.

References

1. C. J. BRINKER and G. W. SCHERER, "Sol–Gel Science: The Physics and Chemistry of Sol–Gel Processing" (Academic Press, New York, 1990).
2. Y.-J. KIM and L. F. FRANCIS, *J. Amer. Ceram. Soc.* **76** (1993) 737.
3. L. F. FRANCIS, *Materials and Manufacturing processes*, **12** (1997) 963.
4. M. A. ANDERSON, M. J. GIESELNANN and Q. XU, *J. Membrane Sci.* **39** (1988) 243.
5. V. T. ZASPALIS, W. VAN PRAAG, K. KEIZER, J. G. VAN OMMEN, A. J. BURGGRAAF and J. R. H. ROSS, *J. Mater. Sci.* **27** (1992) 1023.
6. W. J. KAISER and E. M. LOGOTHETIS, SAE Technical Paper Series, No. 830 167. (Society of Automotive Engineers, Warrendale, PA).
7. C. J. BRINKER, A. J. HURD and K. J. WARD, in "Ultrastructure Processing of Advanced Ceramics", edited by L. L. Hench and D. R. Ulrich (Wiley, New York, 1988) p. 223.
8. S. S. PRAKASH, C. J. BRINKER and A. J. HURD, *J. Non-Cryst. Solids* **190** (1995) 264.
9. K. BANGE, C. R. OTTERMANN, O. ANDERSON, U. JESCHKOWSKI, M. LAUBE and R. FEILE, *Thin Solid Films* **197** (1991) 279.
10. B. E. YOLDAS and T. W. O'KEEFFE, *Appl. Opt.* **18** (1979) 3133.
11. H. DISLICH, in "Sol-Gel Technology for Thin Films, Fibers, Performs, Electronics, and Speciality Shapes", edited by L. C. Klein (Noyes Pub., Park Ridge, NJ, 1988) p. 50.
12. A. TAKAMI, *Amer. Ceram. Soc. Bull.* **67** (1988) 1956.
13. E. HACHFELD, Y.-J. KIM and L. F. FRANCIS, *Mater. Lett.* **18** (1933) 141.
14. Y.-J. KIM, N. M. WARA, B. V. VELAMAKANNI and L. F. FRANCIS, "Ceramic Transactions, Vol. 43: Ferroic Materials: Design, Preparation and Sensor Characteristics", edited by A. S. Bhalla, K. M. Nair, I. K. Lloyd, H. Yanagida and D. A. Payne (American Ceramic Society, Westerville, OH, 1994) p. 183.
15. N. D. S. MOHALLEM and M. A. AEGERTER, *J. Non-Cryst. Solids* **100** (1988) 526.
16. N. ÖZER, *Thin Solid Films* **214** (1992) 17.
17. E. A. BARRINGER and H. K. BOWEN, *Langmuir* **1** (1985) 414.
18. J. H. JEAN and T. A. RING, *ibid.* **2** (1986) 251.
19. J.-L. LOOK and C. F. ZUKOSKI, *J. Amer. Ceram. Soc.* **75** (1992) 1587.
20. J.-L. LOOK, G. H. BOGUSH and C. F. ZUKOSKI, *Faraday Discuss. Chem. Soc.* **90** (1990) 345.
21. M. I. DIAZ-GUEMES, T. G. CARRENO, C. J. SERNA and J. M. PALACIOS, *J. Mater. Sci. Lett.* **7** (1988) 671.
22. J. H. JEAN and T. A. RING, *Amer. Ceram. Soc. Bull.* **66** (1987) 1517.
23. L. H. EDELSON and A. M. GLAESER, *J. Amer. Ceram. Soc.* **71** (1988) 225.
24. B. D. CRAIG, L. F. FRANCIS and L. ABRAMS, *ibid.* **79** (1996) 3317.
25. J. GOWOREK and W. STEFANIAK, *Colloids and Surfaces* **55** (1991) 359.
26. M. E. THOMAS, M. P. HARTNETT and J. E. MCKAY, *J. Vac. Sci. Technol.* **A6** (1988) 2570.
27. G. G. STONEY, *Proc. Roy. Soc. Lond.* **A82** (1949) 172.
28. M. OHRING, "The Materials Science of Thin Films" (Academic Press, New York, 1992).
29. R. GLANG, R. A. HOLMWOOD and R. L. ROSENFELD, *Rev. Sci. Instr.* **36** (1965) 7.
30. C. J. LAWRENCE, *Phys. Fluids* **A2** (1990) 453.
31. PEMBERTON and MASH, *J. Chem. Thermodynam.* **10** (1978) 867.
32. J.-L. LOOK and C. F. ZUKOSKI, *J. Amer. Ceram. Soc.* **78** (1995) 21.
33. K.-N. P. KUMAR, K. KELZER, A. J. BURGGRAAF, T. OKUBO and H. NAGAMOTO, *J. Mater. Chem.* **3** (1993) 1151.
34. K.-N. P. KUMAR, K. KELZER and A. J. BURGGRAAF, *ibid.* **3** (1993) 1141.
35. B. E. YOLDAS, *J. Mater. Sci.* **21** (1986) 1087.
36. K. KATO, T. TSUZUKI, T. TAODA, Y. TORII, T. KATO and Y. BUTSUGAN, *ibid.* **29** (1994) 5911.
37. S. G. CROLL, *J. Appl. Polym. Sci.* **23** (1979) 847.
38. T. J. GARINO and H. K. BOWEN, *J. Amer. Ceram. Soc.* **73** (1990) 251.

Received 12 March 1997
and accepted 24 June 1998